

# Aerosol-Cloud Relationships in Marine Stratocumulus

Yi-Chun Chen<sup>1\*</sup>, Zachary J. Lebo<sup>1</sup>, Lulin Xue<sup>2</sup>, Roy Rasmussen<sup>2</sup>, and John H. Seinfeld<sup>1,3</sup>

<sup>1</sup> Environmental Science and Engineering, California Institute of Technology, Pasadena, CA 91125

<sup>2</sup> National Center for Atmospheric Research, Boulder, CO 80301

<sup>3</sup> Chemical Engineering, California Institute of Technology, Pasadena, CA 91125

## 1 Introduction

Marine stratocumulus clouds (MSc), which cover about 30% of the world's oceans (Warren et al., 1986), are generally optically thick and shallow, exerting a net cooling influence on climate. Perturbations in aerosol affect cloud droplet number concentration (Twomey, 1974) and size distribution, and thereby have an influence on precipitation (Albrecht, 1989), cloud-top entrainment, cloud thickness and adiabaticity. Wood (2007) shows that the MSc cloud thickness response is determined by a balance between the moistening/cooling of the marine boundary layer (MBL) resulting from the suppression of surface precipitation, and the drying/warming resulting from enhanced entrainment due to increased turbulent kinetic energy (TKE). The drying and warming effect (cloud thinning) opposes the moistening/cooling effect (cloud thickening) and can totally cancel it under certain conditions. Drying/warming may result in thinner clouds as cloud droplet number concentration increases. It is also shown that the free troposphere moisture has a strong control on the precipitation rate through cloud-top entrainment, thus altering the balance between the competing effects of precipitation on LWP (Ackerman et al., 2004).

In this study, we focus on the aerosol-cloud-precipitation interactions under different environmental conditions to explore the dynamical effects. We report here on a numerical study of the dynamical response of MSc to aerosol changes using the Weather Research and Forecasting (WRF) model with a detailed bin-resolved microphysical scheme as a three-dimensional large eddy simu-

lation (LES) model. Simulations are performed to explore the cloud thickness response to varying aerosol number concentration ( $N_a=100$  and  $1000\text{ cm}^{-3}$ ) and covarying meteorological conditions (sea surface temperature (SST), free-tropospheric water vapor mixing ratio and large-scale subsidence). Simulations of idealized cases of nocturnal MSc are carried out with a vertical resolution of 20 m and horizontal resolution of 60 m.

## 2 Model Description

In this study, we employ WRF model with detailed bin microphysical scheme as a 3D LES model. The detailed Bin-Resolved microphysical scheme (Geresdi, 1998; Rasmussen et al., 2002; Xue et al., 2010) predicts for both mass and number concentration, which follows the moment-conserving technique (Tzivion et al., 1987). The cloud drops are divided into 36 size bins with radius ranging from  $1.56\text{ }\mu\text{m}$  to  $6.4\text{ }\mu\text{m}$  and with mass doubling every bin. The aerosols are divided into 40 size bins in the radius range  $0.006$  to  $66.2\text{ }\mu\text{m}$ . Aerosol activation is calculated based on Köhler theory. The microphysical processes include aerosol activation, drop condensation/evaporation, collision-coalescence, collisional breakup, sedimentation and regeneration of aerosols. The aerosol regeneration mechanism allows the aerosols to be released by evaporated drops; aerosols are conserved in the domain unless the drops fall to the surface. Cloud droplets are defined as drops with radius  $< 40\text{ }\mu\text{m}$ ; drops with radius  $\geq 40\text{ }\mu\text{m}$  are classified as rain drops.

Other schemes applied in the model include radiation scheme (radiative rapid transfer model RRTM), surface layer scheme (Monin-Obukhov scheme) and turbulence scheme (1.5 order TKE

---

\*Corresponding author address: Yi-Chun Chen, Environmental Science and Engineering, California Institute of Technology, Pasadena, CA 91125; E-mail: ycc@caltech.edu

closure).

### 3 Experimental Design

The aerosol is assumed to be soluble ammonium sulfate with lognormal distribution mean radius  $0.1 \mu\text{m}$  and geometric standard deviation 1.5. The initial sounding profile (Fig. 1) of the control case follows Hill et al. (2009) with wind field  $-1 \text{ m/s}$  in the  $x$ - direction and  $6 \text{ m/s}$  in the  $y$ - direction. The surface pressure is prescribed as  $1000 \text{ hPa}$ . For the nocturnal study, only longwave radiation is considered. The grid resolution is  $20 \text{ m}$  vertically and  $60 \text{ m}$  horizontally, with numerical time step  $0.5 \text{ s}$ . Aerosol number concentration ( $N_a$ )  $100 \text{ cm}^{-3}$  and  $1000 \text{ cm}^{-3}$  correspond to clean and polluted case, respectively. Three significant environmental variables are considered, including SST, free tropospheric water vapor mixing ratio  $q_{FT}$  and large-scale divergence rate  $D$ . The large-scale subsidence is prescribed by  $W_{sub} = -Dz$ , where  $z$  is the height. All simulations listed in Table. 1 are performed in the 3D domain  $2.4 \text{ km} \times 2.4 \text{ km} \times 1.6 \text{ km}$  with  $6\text{hr}$  duration. Both clean and polluted cases are simulated under each condition.

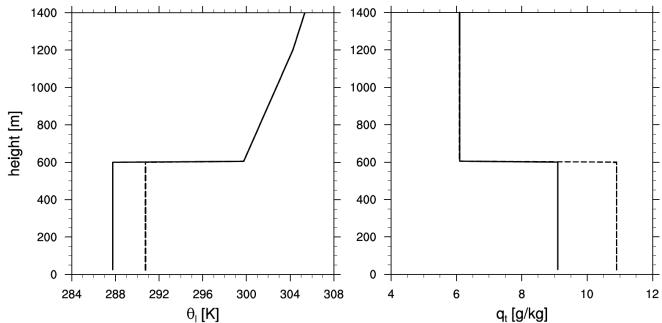


Figure 1: Initial sounding profile (liquid water potential temperature  $\theta_l$  and total water mixing ratio  $q_t$ ) for the MSc. Solid line is the Control run, and dashed line is the SST291 run.

In SST291 run, SST and initial  $\theta_l$  (liquid water potential temperature) are increased by  $3\text{K}$  to study the effect of warmer temperature. The initial  $q_t$  (total water mixing ratio) is adjusted to have the same relative humidity as the Control run (Fig. 1 dashed line); while the free troposphere profile remains the same. In QFT1 run, the free tropospheric water vapor mixing ratio is decreased to  $1.1 \text{ g/kg}$  to study the effect of drier

Table 1: Simulations with varied environmental conditions.

	SST (K)	$q_{FT}$ (g/kg)	D (1/s)
Control	288	6.1	$5.5 \times 10^{-6}$
SST291	291	6.1	$5.5 \times 10^{-6}$
QFT1	288	1.1	$5.5 \times 10^{-6}$
DIV3	288	6.1	$3.0 \times 10^{-6}$

free troposphere to MSc; the temperature profile remains unchanged.

## 4 Results

### 4.1 Control Run

For the clean case ( $N_a = 100 \text{ cm}^{-3}$ ), the surface precipitation increases after  $3\text{hr}$  acting as a sink of moisture (Fig. 2), causing the LWP and cloud thickness to decrease with time. Sub-cloud rain re-evaporation results in moistening and cooling in the subcloud layer, weaker turbulence intensity, less entrainment, and reduced LWP (Fig. 3).

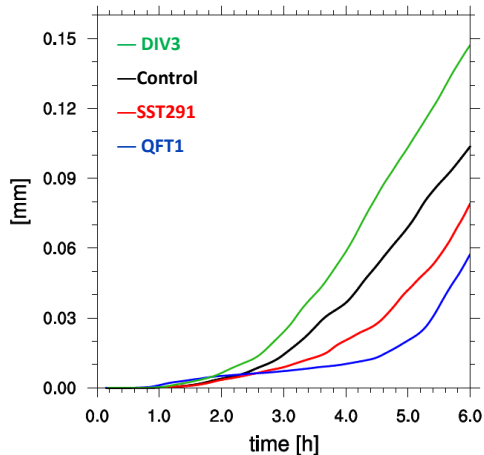


Figure 2: Surface accumulated precipitation in the clean cases ( $N_a=100 \text{ cm}^{-3}$ ); no precipitation is generated in the polluted cases.

On the other hand, increase in aerosol ( $N_a=1000 \text{ cm}^{-3}$ ) results in higher cloud droplet number concentration  $N_d$  but with smaller size (Fig. 4). The numerous and smaller droplets have less efficient collision-coalescence, which suppresses the precipitation and increases the LWP. Decreased surface precipitation leads to acceleration of cloud-top entrainment because less evaporative cooling below cloud increases the TKE to

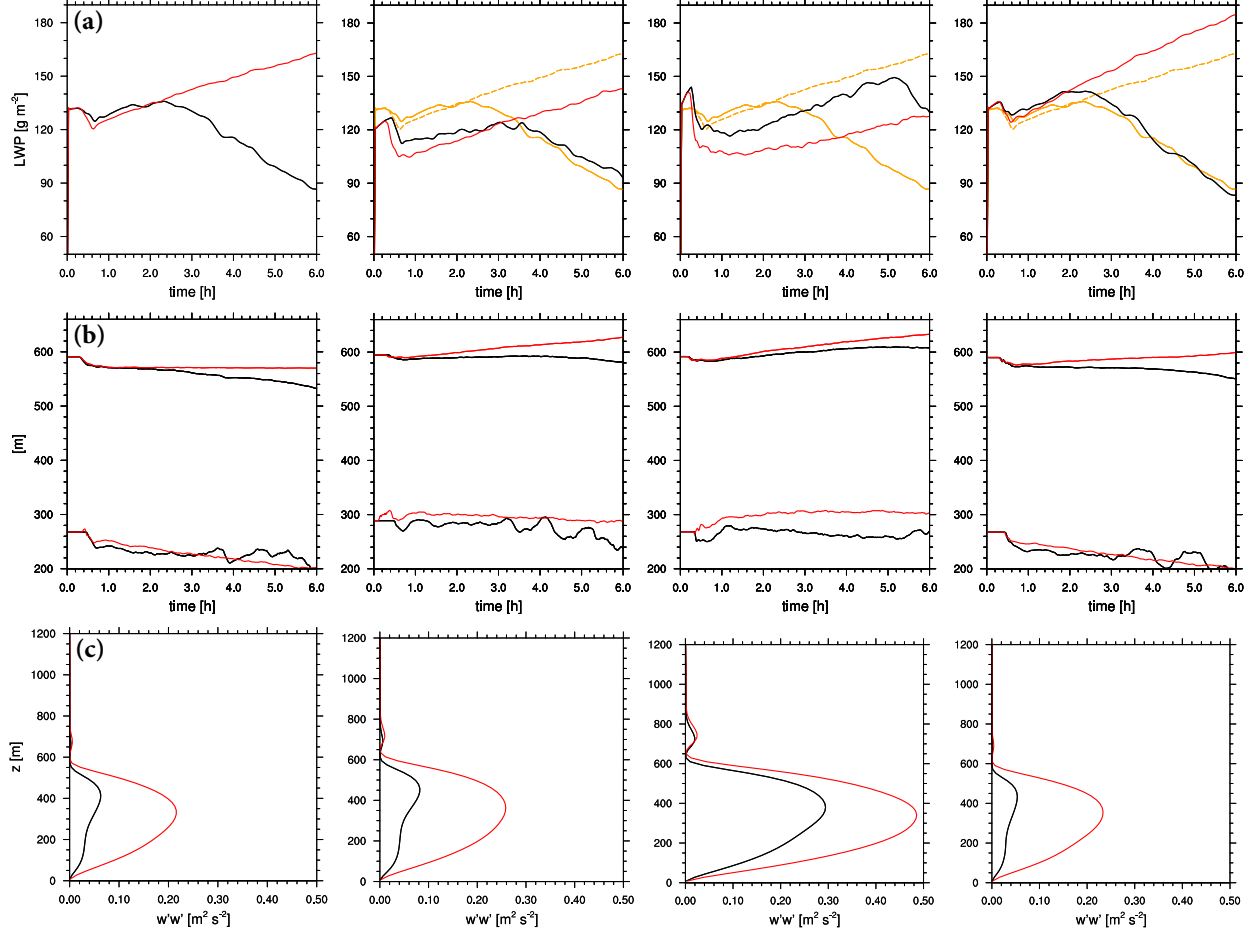


Figure 3: The four columns correspond to Control, SST291, QFT1 and DIV3 simulations, respectively. The black line is the clean case, and the red line is the polluted case. The rows are: (a) time evolution of horizontally averaged LWP [ $\text{g}/\text{m}^3$ ]. The yellow solid line and dashed line correspond to clean and polluted case in the Control run, for comparison. (b) time evolution of horizontally averaged cloud top and base height [unit:m], defined as averaged cloud water mixing ratio  $\geq 0.01$  g/kg. (c) vertical profile of the vertical velocity variance averaged over the last 3 hr.

drive cloud-top entrainment, thus destabilizing the MBL. In the vertical profile of vertical velocity variance (Fig. 3c), it is shown that the turbulence strength is much weaker in the precipitating cloud than the non-precipitating cloud, in agreement with Ackerman et al. (2004), that the entrainment rate increases with  $N_a$  in all simulations (Fig. 5b).

## 4.2 SST291 Run

The varying SST primarily affects the lower tropospheric stability. With higher temperature in the MBL with warmer SSTs, both cloud base and top increase in height because of a weaker temperature inversion and thus stronger entrainment (Fig. 3).

Comparing with the Control run, the higher entrainment rate causes the clean case precipitation to decrease and LWP to increase slightly. In the polluted case, increased entrainment results in stronger drying/warming effect in the cloud and lower LWP than in the Control run. When the temperature increases in MBL, the cloud thins due to cloud base rising faster than cloud top.

## 4.3 QFT1 Run

With drier entrained air, the clean case precipitation decrease significantly compared to the Control run (Fig. 2), resulting in higher LWP. For the polluted case, cloud-top entrainment leads to stronger drying and lower LWP. LWP is higher in

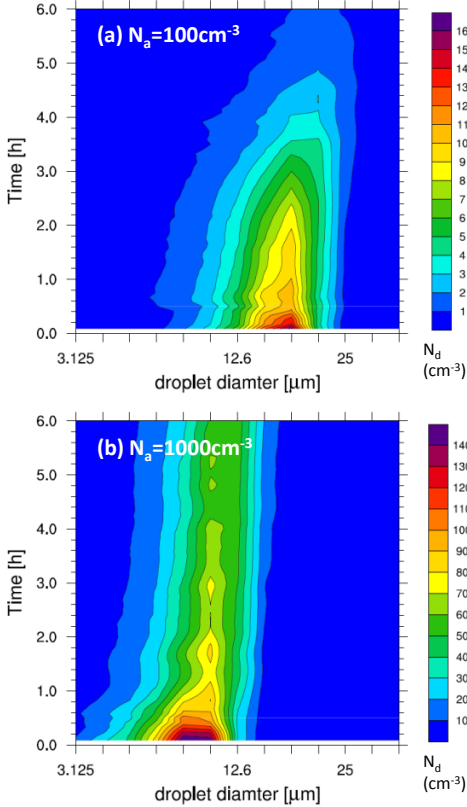


Figure 4: Temporal evolution of cloud droplet spectrum averaged over the domain for (a) clean and (b) polluted case in the Control run.

the clean case than in the polluted case within the 6hr duration. This indicates that with increasing  $N_a$ , the drying/warming effect from entrainment surmounts the moistening/cooling effect from suppressed precipitation.

In the polluted case, the average cloud-top entrainment rate is the highest among all (Fig. 5). This is caused by evaporation-entrainment and sedimentation-entrainment feedback (Hill et al., 2009). The drier entrained air leads to more rapid evaporation in the cloud-top entrainment zone. This reduces the LWP, suppressing the surface precipitation, and causing stronger TKE through increased cloud-top evaporative cooling. Both precipitation suppression and evaporation enhancement near cloud top result in higher TKE and entrainment rate, and further drying.

#### 4.4 DIV3 Run

The large-scale divergence rate determines the subsidence rate and affects the cloud top height.

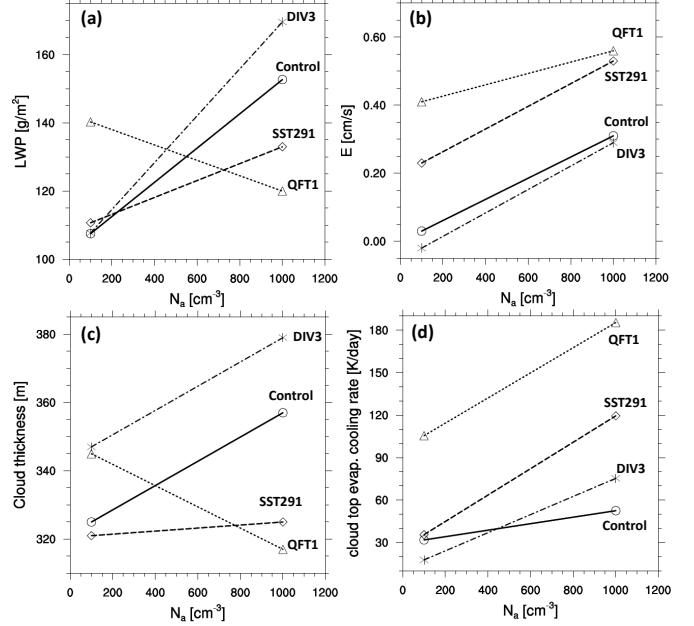


Figure 5: The last 3 hr averaged values of (a) LWP, (b) entrainment rate, calculated based on  $E = dz_i/dt + Dz_i$ , where  $z_i$  is cloud top height, (c) cloud thickness, and (d) cloud top evaporative cooling rate. The symbols correspond to clean and polluted cases, respectively.

As the large-scale divergence decreases, the cloud top is driven higher, thickening the cloud. This results in more precipitation in the clean case and thicker cloud/higher LWP in the polluted case. Entrainment is weaker in this scenario due to weaker large-scale subsidence.

## 5 Conclusions

Simulations of varying aerosol number concentration and environmental variables are carried out using the WRF model with a detailed bin microphysical scheme. It is shown that heavy precipitation leads to a reduction in cloud thickness and entrainment. As aerosol increases, the suppression of precipitation results in thicker cloud and stronger entrainment. However, increased aerosol in a light drizzling cloud results in cloud thinning due to a relatively stronger drying/warming effect. It is found the competition between precipitation and entrainment in MSc is sensitive to both aerosol concentration and environmental conditions.

## References

- Ackerman, A. S., Kirkpatrick, M. P., Stevens, D. E., and Toon, O. B.: The impact of humidity above stratiform clouds on indirect aerosol climate forcing, *Nature*, 432, 1014–1017, 2004.
- Albrecht, B.: Aerosols, Cloud Microphysics, and Fractional Cloudiness, *Science*, 245, 1227–1230, doi:10.1126/science.245.4923.1227, 1989.
- Geresdi, I.: Idealized simulation of the Colorado hailstorm case: comparison of bulk and detailed microphysics, *Atmos. Res.*, 45, 237–252, 1998.
- Hill, A. A., Feingold, G., and Jiang, H.: The influence of entrainment and mixing assumption on aerosol-cloud interactions in marine stratocumulus, *J. Atmos. Sci.*, 66, 1450–1464, 2009.
- Rasmussen, R. M., Geresdi, I., Thompson, G., Manning, K., and Karplus, E.: Freezing Drizzle Formation in Stably Stratified Layer Clouds: The Role of Radiative Cooling of Cloud Droplets, Cloud Condensation Nuclei, and Ice Initiation, *J. Atmos. Sci.*, 59, 837–860, 2002.
- Twomey, S.: Pollution and the Planetary Albedo, *Atmos. Environ.*, 8, 1251–1256, 1974.
- Tzivion, S., Feingold, G., and Levin, Z.: An Efficient Numerical Solution to the Stochastic Collection Equation, *J. Atmos. Sci.*, 44, 3139–3149, 1987.
- Warren, S. G., Hahn, C. J., London, J., Chervine, R. M., , and Jenne, R. L.: Warren, S. G., C. J. Hahn, J. London, R. M. Chervine, and R. L. Jenne, NCAR/TN-317 STR, NCAR Tech. Note., p. 29, 1986.
- Wood, R.: Cancellation of aerosol indirect effects in marine stratocumulus through cloud thinning, *J. Atmos. Sci.*, 64, 2657–2669, doi: 10.1175/JAS3942.1, 2007.
- Xue, L., Teller, A., Rasmussen, R. M., Geresdi, I., and Pan, Z.: Effects of aerosol solubility and regeneration on warm-phase orographic clouds and precipitation simulated by a detailed bin microphysical scheme, *J. Atmos. Sci.*, doi: 10.1175/2010JAS3511.1, 2010.